



## X-ray detectors for the BabyIAXO solar axion search

K. Altenmüller <sup>a,\*</sup>, B. Biasuzzi <sup>c</sup>, J.F. Castel <sup>a</sup>, S. Cebrián <sup>a</sup>, T. Dafni <sup>a</sup>, K. Desch <sup>d</sup>, D. Díez-Ibañez <sup>a</sup>, E. Ferrer-Ribas <sup>c</sup>, J. Galan <sup>a</sup>, J. Galindo <sup>a</sup>, J.A. García <sup>a</sup>, I.G. Irastorza <sup>a</sup>, J. Kaminski <sup>d</sup>, G. Luzón <sup>a</sup>, C. Margalejo <sup>a</sup>, H. Mirallas <sup>a</sup>, X.F. Navick <sup>c</sup>, L. Obis <sup>a</sup>, A. Ortiz de Solórzano <sup>a</sup>, J. von Oy <sup>d</sup>, T. Papaevangelou <sup>c</sup>, O. Pérez <sup>a</sup>, J. Ruz <sup>a</sup>, T. Schiffer <sup>d</sup>, S. Schmidt <sup>d</sup>, L. Segui <sup>c</sup>, J.K. Vogel <sup>a,b</sup>

<sup>a</sup> Center for Astroparticles and High Energy Physics (CAPA), Universidad de Zaragoza, Zaragoza, 50009, Spain

<sup>b</sup> LLNL Lawrence Livermore National Laboratory, Livermore, 94550, USA

<sup>c</sup> IRFU, CEA, Université Paris-Saclay, Gif-sur-Yvette, 91191, France

<sup>d</sup> Physikalisches Institut der Universität Bonn, Bonn, 53115, Germany



### ARTICLE INFO

#### Keywords:

X-ray detectors

Micropattern gaseous detectors

Dark matter detectors

### ABSTRACT

BabyIAXO is a helioscope under construction to search for an emission of the axion particle from the Sun. At the same time it serves as an intermediate stage towards the International Axion Observatory (IAXO). An integral component of this experiment is a low background X-ray detector with a high efficiency in the 1–10 keV energy range. Micromegas detectors are considered as baseline technology for BabyIAXO thanks to the relatively high efficiency and very low background level. Other detector technologies developed to reach better energy resolution while maintaining high efficiency and low background level are also under study. In this paper, we review the BabyIAXO design and present the analysis of data taken with the prototype of an IAXO Micromegas detector. A background level of  $8.8 \times 10^{-7}$  counts  $\text{keV}^{-1} \text{cm}^{-2} \text{s}^{-1}$  was reached.

### 1. Introduction

BabyIAXO is a helioscope under construction, which will search for an emission of hypothetical axion particles (and axion-like particles) from the Sun [1,2]. The axion is theoretically well motivated — it arises when the Peccei–Quinn mechanism is used to solve the strong CP problem [3,4]. Axions couple to photons, which permits the transformation of axions into photons via the Primakoff effect — and vice versa. In addition, non-hadronic axion models also predict a significant coupling of axions to electrons [e.g. 5,6]. Simple models predicting relatively heavy axions were already ruled out, thus if this particle exists, it has to be very light and have a low interaction strength [7]. These properties make the axion a well-suited dark matter candidate [8]. In addition, there are several hints from astrophysical observations that dark matter indeed might consist of axions. For example, observations of a too fast cooling of white dwarfs and an anomalous transparency of the universe to very high-energy gamma rays could be explained by axion–photon oscillations [9–11]. The region of the parameter space motivated by both white dwarfs and the transparency hint is partially in reach for a next-generation helioscope like BabyIAXO [1].

A full review of the physics case relevant for BabyIAXO can be found in the Ref. [12].

### 2. The BabyIAXO helioscope

The principle of an axion helioscope is the following: a strong magnet with a large volume is pointed at the Sun. Due to the large density of virtual photons within this volume, axions coming from the Sun can transform into X-ray photons via the inverse Primakoff effect. At the end of the magnet, X-ray optics focus the resulting photons onto ultra-low background detectors [13]. The discovery potential of such a setup is defined by several parameters, which one intends to maximize: the strength, length and volume of the magnet, the throughput of the optics and smallness of the focal spot, the efficiency and background level in the region of interest in the detector as well as the exposure time tracking the Sun [1]. Even though BabyIAXO is a fully-fledged helioscope that will explore relevant parameter space, it is considered a prototype for an even larger experiment — IAXO, the International AXion Observatory [2,14]. At the same time, BabyIAXO builds on experience made with the CERN Axion Solar Telescope (CAST), which took data until the end of 2021 and delivered current benchmark limits over a wide range in the axion parameter space which are at the same level as astrophysical limits [15].

BabyIAXO is going to be constructed at DESY in Hamburg, Germany, and commissioning is expected to start in 2026. Following

\* Corresponding author.

E-mail address: [konrad.altenmueller@unizar.es](mailto:konrad.altenmueller@unizar.es) (K. Altenmüller).

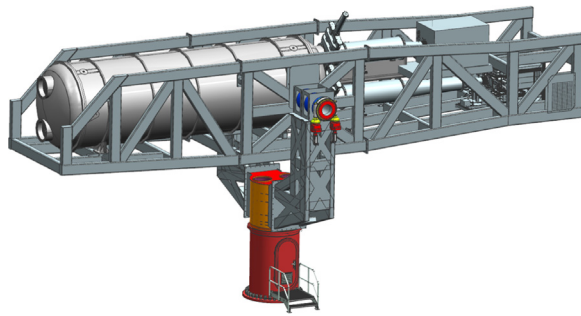


**Fig. 1.** A sketch of the BabyIAXO helioscope. Mounted in a frame on the drive system, one can see the cryostat containing the magnet on the left, connected on the right to the X-ray telescopes and the detectors within their veto-systems. The total length of the helioscope is  $\sim 21$  m.

developments are currently in progress:

- Magnet: it is planned to use a 10 m long double racetrack-coil design made of a superconducting Al-stabilized Nb-Ti/Cu Rutherford cable that can provide a maximum magnetic field of 4 T. Two empty bores with each 70 cm diameter go through the entire length of the common coil. The average magnetic field within the volume will be between 2 and 3 T. A cryostat will house the magnet and keep the cold mass at 4.5 K.
- X-ray optics: two different Wolter telescopes will be used for BabyIAXO [16]. One of them is a flight spare telescope of ESA's XMM Newton mission [17], the other is a custom design, drawing from developments for NuSTAR, Athena and XRISM [18–20]. The goal is to focus the X-ray signal onto a spot of less than 2.5 mm radius on the detector located in the focal plane.
- Drive system: the drive system will be able to rotate the helioscope, and to tilt it by  $21^\circ$  below and above the horizon, which from the geographical location of DESY allows to track the Sun for 50% of the time. While dealing with a load of up to 90 t, the system will keep a pointing precision of better than  $0.01^\circ$ .
- The X-ray detectors, which are the final element in the chain to detect axions, are described in detail in the next section.

A conceptual sketch of the current BabyIAXO design is shown in Fig. 1. For more information, the design of BabyIAXO is presented in great detail in the paper [1].

### 3. Low background X-ray detectors for BabyIAXO and beyond

The expected energy spectrum of solar axions converted into photons within the BabyIAXO magnet volume can be computed, showing a distribution with a peak at  $\sim 1$  keV (depending on the exact model) and a tail that extends to  $\sim 10$  keV [5]. Thus a detector with a low threshold and a high detection efficiency in the 1–10 keV region is necessary. Due to the expected rareness of events, a background level as low as possible is required. In the baseline design it is intended to use a Micromegas detector. In addition, further detectors are under development for later stages of data acquisition, but so far none was able to demonstrate a background level as low as achievable with the Micromegas detector. The different detectors are listed in the following:

- Micromegas: a Micromegas detector is a gas-filled time projection chamber with a pixelated readout structure [21]. The thickness of the chamber volume is 3 cm, while the read-out covers a surface of  $6 \times 6$  cm $^2$  with 120 strips in each direction. A mesh is placed just 50  $\mu$ m above the readout and kept at a high voltage, creating a drift region with the cathode, which doubles as entrance window, and an amplification region with the strip readout, which serves as anode. A detector of this type is produced via the

microbulk method using only radiopure copper and kapton [22]. Employing an appropriate gas mixture and pressure, a detection efficiency of 60%–70% is reached in the region of interest. The detector threshold is  $\sim 1$  keV and mostly limited by the thickness of the entrance window. The IAXO collaboration is working on developing a few hundred nm thick silicon nitride windows to improve the overall threshold. Furthermore, the use of xenon-based gas mixtures allows the implementation of thinner windows, as a good detection efficiency is reached at lower pressures as with argon. A Micromegas detector was used at BabyIAXO's predecessor, the CAST experiment, where a background level of  $1 \times 10^{-6}$  counts keV $^{-1}$  cm $^{-2}$  s $^{-1}$  was reached [23].

- GridPix: the GridPix detector is an evolution of the Micromegas, where each hole in the mesh is read out by a single pixel of a CMOS chip, utilizing the TimePix3 chip [24,25]. This detector allows single electron detection, a complete 3-dimensional reconstruction of the initial charge cloud, and a dead time-free read-out. A GridPix detector was used at CAST in 2014–2015 and achieved a background level of  $\sim 10^{-5}$  counts keV $^{-1}$  cm $^{-2}$  s $^{-1}$  [24].
- Silicon drift detectors (SDDs): SDDs are semiconductor detectors with a point-like anode, resulting in a low capacity of the detector, which in turn improves the detector performance and allows an energy resolution of  $\sim 130$  eV at 6 keV. The advantage of these detectors is that they do not require cryogenics. A setup with SDDs would not need a window like for gas-filled detectors, which makes it possible to achieve an energy threshold of  $< 500$  eV [26]. Simulations based on measurements show that a background level in the order of  $\sim 10^{-6}$  counts keV $^{-1}$  cm $^{-2}$  s $^{-1}$  is within reach [1].
- Metallic magnetic calorimeters (MMCs): this detector consists of an array of typically 64 pixels operated at a temperature  $< 100$  mK. The heat produced by radiation in an absorber leads to an temperature increase, which induces a change of magnetization of a paramagnetic sensor sitting in a static magnetic field. This change of magnetization can be read out using superconducting pickup coils coupled to dc-SQUIDs. This type of detector features a very high efficiency and an excellent energy resolution in the few eV range which would allow for axion spectroscopy once detection is confirmed. In a setup without any shielding above ground a background level of  $3 \times 10^{-4}$  counts keV $^{-1}$  cm $^{-2}$  s $^{-1}$  was determined [27].

More details and further detectors that are under consideration for this project are described in the BabyIAXO design paper [1].

### 4. The IAXO-D0 detector prototype setup

At the University of Zaragoza, a Micromegas prototype detector, dubbed IAXO-D0, is installed and taking background data in order to characterize it under different conditions and to improve the background rejection. The Micromegas is placed inside a lead shielding of 20 cm thickness. This lead castle is surrounded by a veto system, consisting of three layers of plastic scintillators. Cadmium sheets are placed between and around the scintillators to capture neutrons. This design approach was chosen to attempt not only the rejection of background signals induced by muons, but also by cosmogenic neutrons. Both the Micromegas and the vetoes are read out by a total of 8 AGET ASICs [28]. A gas system recirculates the detector gas and allows pressure and flow to be selected. In our measurements the mixtures Ar (97.7%) + C<sub>4</sub>H<sub>10</sub> (2.3%) and Xe (48.85%) + Ne (48.85%) + C<sub>4</sub>H<sub>10</sub> (2.3%) were used. The isobutane (C<sub>4</sub>H<sub>10</sub>) serves as a quencher. The system is calibrated with a <sup>55</sup>Fe-source. The source is moved by a remote controlled manipulator, connected to the evacuated volume in front of the entrance window, thus it is not required to open the veto for each calibration.

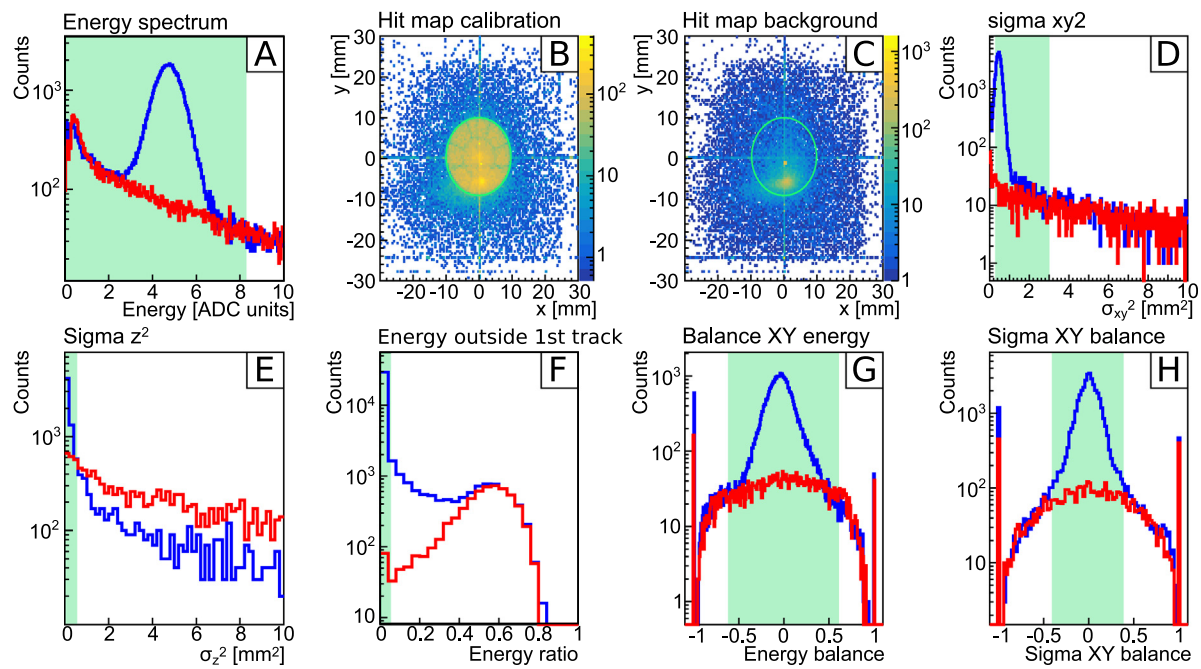


**Fig. 2.** These plots compare data obtained with the  $^{55}\text{Fe}$  calibration-source (blue histograms) and background runs (red histograms). The shaded area indicates the cuts applied to each observable. All events outside the shaded areas are removed from the data. **A:** energy. The 5.9 keV peak is clearly visible in the calibration data; **B, C:** calibration and background hit maps, respectively. The rings mark the fiducial area with radius 1 cm. In the calibration data, the shadow of the entrance window strongback is visible; **D:**  $\sigma_{xy}^2$ , a measure of the size of the energy deposit projected onto the readout plane; **E:**  $\sigma_z^2$ , a measure of the temporal length of the signal, i.e. the spread in the z direction; **F:** fraction of energy outside the first track of an event; **G:** symmetry of the energy in the charge deposit; **H:** symmetry of the charge deposit in space.

## 5. Data analysis and characterization results

The analysis of the data acquired with the Micromegas detector is processed and analyzed using the REST-for-Physics software framework [29]. This software processes the signals from the strips and extracts spectra and 3-dimensional topological information of the charge deposition. The multitude of observables extracted from each event allows to define cuts which result in a very efficient background rejection. The signature of an axion-like signal is determined by the 5.9 keV X-rays of the  $^{55}\text{Fe}$ -source. In general, a low energy X-ray is expected to leave a small, symmetrical charge deposit in the detector. In the context of BabyIAXO, the signals of interest are located in a small spot in the center of the detector read-out plane — the focal spot of the telescope.

The data presented here was obtained by using the same Micromegas, which was previously installed at CAST, and using the Xe–Ne gas mixture. Fig. 2 shows a comparison of observables of calibration and background data and illustrates the cuts applied. These cuts were optimized by maximizing the number of calibration events preserved, while minimizing the number of events preserved in the background data. In addition, a veto cut is applied to remove muon events that managed to slip through the previous cuts. Combining several background runs, 63 of initially 542 243 events pass all the cuts. The total number of events was accumulated over the duration of 26 effective days of data taking within the fiducial area of the detector. The remaining number of counts corresponds to a background level of  $8.8 \times 10^{-7}$  counts  $\text{keV}^{-1} \text{cm}^{-2} \text{s}^{-1}$ . The efficiency of the cuts applied is 49.8%, meaning that they remove also half of the calibration events. This low efficiency can be explained by issues in the data quality, caused by noisy spots in the read-out (see the hitmaps in Fig. 2) and the topological separation of the charge deposit due to several dead strips.

## 6. Conclusions and future developments

In this paper we presented measurements with a Micromegas detector, demonstrating a background level of  $8.8 \times 10^{-7}$  counts  $\text{keV}^{-1}$

$\text{cm}^{-2} \text{s}^{-1}$ . The goal of the detector development is to reduce the background level even more to  $1 \times 10^{-7}$  counts  $\text{keV}^{-1} \text{cm}^{-2} \text{s}^{-1}$ . To achieve this, a second Micromegas prototype setup is under commissioning at the Canfranc underground laboratory (LSC). This setup will help to understand the contributions of cosmogenic and terrestrial background sources better. In addition, radiopure electronics were developed and will be used with the new prototype detectors. With the data presented above, the veto system was not used up to its full potential (apart from cutting muon events). First studies using more advanced cuts depending on signal multiplicity and timing in the vetoes show already an improvement in the background rejection. Software updates and accurate Montecarlo simulations are in progress and will allow us to better understand the signature of neutron-induced background and to define more complex cuts using the veto.

## Acknowledgments

We acknowledge support from the European Research Council (ERC) under the European Union's Horizon 2020 research and innovation programme, grant agreement ERC-2017-AdG788781 (IAOX+) as well as ERC-2018-StG-802836 (AxScale), and from the Spanish Agencia Estatal de Investigación under grant FPA2016-76978-C3-1-P, the coordinated grant PID2019-108122 GB, and the María de Maeztu grant CEX2019-000918-M. Part of this work was performed under the auspices of the U.S. Department of Energy by Lawrence Livermore National Laboratory under Contract DE-AC52-07NA27344. J.A. García acknowledges support from the Juan de la Cierva-Incorporacion program (IJCI2019-040686-I) from the Spanish Ministry of Science and Innovation.

## References

- [1] A. Abeln, K. Altenmüller, S.A. Cuendis, E. Armengaud, D. Attié, S. Aune, S. Basso, L. Bergé, B. Biasuzzi, P.T.C.B. De Sousa, P. Brun, N. Bykovskiy, D. Calvet, J.M. Carmona, J.F. Castel, S. Cebríán, V. Chernov, F.E. Christensen, M.M. Civitani, C. Cogollos, T. Dafní, A. Derbin, K. Desch, D. Díez, M. Dinter, B. Döbrich, I. Drachnev, A. Dudarev, L. Dumoulin, D.D.M. Ferreira, E. Ferrer-Ribas, I. Fleck,

- J. Galán, D. Gascón, L. Gastaldo, M. Giannotti, Y. Giomataris, A. Giuliani, S. Glinenko, J. Golm, N. Golubev, L. Hagge, J. Hahn, C.J. Hailey, D. Hengstler, P.L. Henriksen, T. Houdy, R. Iglesias-Marzoa, F.J. Igua, I.G. Irastorza, C. Iñiguez, K. Jakovcic, J. Kaminski, B. Kanoute, S. Karstensen, L. Kravchuk, B. Lakic, T. Lasserre, P. Laurent, O. Limousin, A. Lindner, M. Loidl, I. Lomskaya, G. López-Alegre, B. Lubsandorzhiev, K. Ludwig, G. Luzón, C. Malbrunot, C. Margalejo, A. Marin-Franch, S. Marnieros, F. Marutzky, J. Mauricio, Y. Meneguén, M. Mentink, S. Mertens, F. Mescia, J. Miralda-Escudé, H. Mirallas, J.P. Mols, V. Muratova, X.F. Navick, C. Nones, A. Notari, A. Nozik, L. Obis, C. Oriol, F. Orsini, A.O. de Solórzano, S. Oster, H.P.P. Da Silva, V. Pantuev, T. Papaevangelou, G. Pareschi, K. Perez, O. Pérez, E. Picatoste, M.J. Pivovaroff, D.V. Poda, J. Redondo, A. Ringwald, M. Rodrigues, F. Rueda-Teruel, S. Rueda-Teruel, E. Ruiz-Choliz, J. Ruz, E.O. Saemann, J. Salvado, T. Schiffer, S. Schmidt, U. Schneekloth, M. Schott, L. Segui, F. Tavecchio, H.H.J.T. Kate, I. Tkachev, S. Troitsky, D. Unger, E. Unzhakov, N. Ushakov, J.K. Vogel, D. Voronin, A. Weltman, U. Werthenbach, W. Wuensch, A. Yanes-Díaz, Conceptual design of BabyIAXO, the intermediate stage towards the international Axion observatory, 2020, <http://dx.doi.org/10.48550/ARXIV.2010.12076>, arXiv URL <https://arxiv.org/abs/2010.12076>.
- [2] E. Armengaud, F.T. Avignone, M. Betz, P. Brax, P. Brun, G. Cantatore, J.M. Carmona, G.P. Carosi, F. Caspers, S. Caspi, S.A. Cetin, D. Chelouche, F.E. Christensen, A. Dael, T. Dafni, M. Davenport, A.V. Derbin, K. Desch, A. Diago, B. Döbrich, I. Dratchnev, A. Dudarev, C. Eleftheriadis, G. Fanourakis, E. Ferrer-Ribas, J. Galán, J.A. García, J.G. Garza, T. Geralis, B. Gimeno, I. Giomataris, S. Glinenko, H. Gómez, D. González-Díaz, E. Guendelman, C.J. Hailey, T. Hiramatsu, D.H.H. Hoffmann, D. Horns, F.J. Igua, I.G. Irastorza, J. Isern, K. Imai, A.C. Jakobsen, J. Jaeckel, K. Jakovčić, J. Kaminski, M. Kawasaki, M. Karuza, M. Krčmar, K. Kousouris, C. Krieger, B. Lakić, O. Limousin, A. Lindner, A. Liolios, G. Luzón, S. Matsuki, V.N. Muratova, C. Nones, I. Ortega, T. Papaevangelou, M.J. Pivovaroff, G. Raffelt, J. Redondo, A. Ringwald, S. Russenschuck, J. Ruz, K. Saikawa, I. Savvidis, T. Sekiguchi, Y.K. Semertzidis, I. Shilon, P. Sikivie, H. Silva, H. ten Kate, A. Tomas, S. Troitsky, T. Vafeiadis, K. van Bibber, P. Vedrine, J.A. Villar, J.K. Vogel, L. Walckiers, A. Weltman, W. Wester, S.C. Yıldız, K. Zioutas, Conceptual design of the international Axion observatory (IAXO), *J. Instrum.* 9 (05) (2014) T05002, <http://dx.doi.org/10.1088/1748-0221/9/05/T05002>.
- [3] R.D. Peccei, H.R. Quinn, CP Conservation in the presence of pseudoparticles, *Phys. Rev. Lett.* 38 (1977) 1440–1443, <http://dx.doi.org/10.1103/PhysRevLett.38.1440>, URL <https://link.aps.org/doi/10.1103/PhysRevLett.38.1440>.
- [4] R.D. Peccei, H.R. Quinn, Constraints imposed by CP conservation in the presence of pseudoparticles, *Phys. Rev. D* 16 (1977) 1791–1797, <http://dx.doi.org/10.1103/PhysRevD.16.1791>, URL <https://link.aps.org/doi/10.1103/PhysRevD.16.1791>.
- [5] J. Redondo, Solar axion flux from the axion-electron coupling, *J. Cosmol. Astropart. Phys.* 2013 (12) (2013) 008, <http://dx.doi.org/10.1088/1475-7516/2013/12/008>.
- [6] S. Hoof, J. Jaeckel, L.J. Thormaehlen, Quantifying uncertainties in the solar axion flux and their impact on determining axion model parameters, *J. Cosmol. Astropart. Phys.* 09 (2021) 006, <http://dx.doi.org/10.1088/1475-7516/2021/09/006>, arXiv:2101.08789.
- [7] J.E. Kim, Light pseudoscalars, particle physics and cosmology, *Phys. Rep.* 150 (1) (1987) 1–177, [http://dx.doi.org/10.1016/0370-1573\(87\)90017-2](http://dx.doi.org/10.1016/0370-1573(87)90017-2), URL <https://www.sciencedirect.com/science/article/pii/0370157387900172>.
- [8] F. Chadha-Day, J. Ellis, D.J.E. Marsh, Axion dark matter: What is it and why now? *Sci. Adv.* 8 (8) (2022) eabj3618, <http://dx.doi.org/10.1126/sciadv.abbj3618>, arXiv:<https://www.science.org/doi/pdf/10.1126/sciadv.abbj3618>.
- [9] J. Isern, E. García-Berro, S. Torres, S. Catalán, Axions and the cooling of white Dwarf stars, *Astrophys. J.* 682 (2) (2008) L109–L112, <http://dx.doi.org/10.1086/591042>.
- [10] L. Di Luzio, M. Fedele, M. Giannotti, F. Mescia, E. Nardi, Stellar evolution confronts axion models, *J. Cosmol. Astropart. Phys.* 02 (02) (2022) 035, <http://dx.doi.org/10.1088/1475-7516/2022/02/035>, arXiv:2109.10368.
- [11] M. Meyer, D. Horns, M. Raue, First lower limits on the photon-axion-like particle coupling from very high energy gamma-ray observations, *Phys. Rev. D* 87 (2013) 035027, <http://dx.doi.org/10.1103/PhysRevD.87.035027>, URL <https://link.aps.org/doi/10.1103/PhysRevD.87.035027>.
- [12] E. Armengaud, D. Attié, S. Basso, P. Brun, N. Bykovskiy, J. Carmona, J. Castel, S. Cebrián, M. Cicoli, M. Civitani, C. Cogollos, J. Conlon, D. Costa, T. Dafni, R. Daido, A. Derbin, M. Descalle, K. Desch, I. Dratchnev, B. Döbrich, A. Dudarev, E. Ferrer-Ribas, I. Fleck, J. Galán, G. Galanti, L. Garrido, D. Gascon, L. Gastaldo, C. Germani, G. Ghisellini, M. Giannotti, I. Giomataris, S. Glinenko, N. Golubev, R. Graciani, I. Irastorza, K. Jakovčić, J. Kaminski, M. Krčmar, C. Krieger, B. Lakić, T. Lasserre, P. Laurent, O. Limousin, A. Lindner, I. Lomskaya, B. Lubsandorzhiev, G. Luzón, M.C.D. Marsh, C. Margalejo, F. Mescia, M. Meyer, J. Miralda-Escudé, H. Mirallas, V. Muratova, X. Navick, C. Nones, A. Notari, A. Nozik, A.O. de Solórzano, V. Pantuev, T. Papaevangelou, G. Pareschi, K. Perez, E. Picatoste, M. Pivovaroff, J. Redondo, A. Ringwald, M. Roncadelli, E. Ruiz-Choliz, J. Ruz, K. Saikawa, J. Salvadó, M. Samperiz, T. Schiffer, S. Schmidt, U. Schneekloth, M. Schott, M. Schott, H. Silva, G. Tagliaferri, F. Takahashi, F. Tavecchio, H. ten Kate, I. Tkachev, S. Troitsky, E. Unzhakov, P. Vedrine, J. Vogel, C. Weinsheimer, A. Weltman, W. Yin, Physics potential of the international Axion observatory (IAXO), *J. Cosmol. Astropart. Phys.* 2019 (06) (2019) 047, <http://dx.doi.org/10.1088/1475-7516/2019/06/047>.
- [13] P. Sikivie, Experimental tests of the "invisible" Axion, *Phys. Rev. Lett.* 51 (1983) 1415–1417, <http://dx.doi.org/10.1103/PhysRevLett.51.1415>, URL <https://link.aps.org/doi/10.1103/PhysRevLett.51.1415>.
- [14] I. Irastorza, F. Avignone, S. Caspi, J. Carmona, T. Dafni, M. Davenport, A. Dudarev, G. Fanourakis, E. Ferrer-Ribas, J. Galán, J. García, T. Geralis, I. Giomataris, H. Gómez, D. Hoffmann, F. Igua, K. Jakovčić, M. Krčmar, B. Lakić, G. Luzón, M. Pivovaroff, T. Papaevangelou, G. Raffelt, J. Redondo, A. Rodríguez, S. Russenschuck, J. Ruz, I. Shilon, H.T. Kate, A. Tomás, S. Troitsky, K. van Bibber, J. Villar, J. Vogel, L. Walckiers, K. Zioutas, Towards a new generation axion helioscope, *J. Cosmol. Astropart. Phys.* 2011 (06) (2011) 013, <http://dx.doi.org/10.1088/1475-7516/2011/06/013>.
- [15] CAST Collaboration, V. Anastassopoulos, et al., New CAST Limit on the Axion-Photon Interaction, *Nat. Phys.* 13 (2017) 584–590, <http://dx.doi.org/10.1038/nphys4109>, arXiv:1705.02290.
- [16] H. Wolter, Spiegelsysteme streifenden Einfalls als abbildende Optiken für Röntgenstrahlen, *Ann. Physics* 10 (1952) 94.
- [17] F. Jansen, et al., XMM-Newton observatory. I. The spacecraft and operations, *Astron. Astrophys.* 365 (2001) L1–L6, <http://dx.doi.org/10.1051/0004-6361:20000036>.
- [18] F.A. Harrison, W.W. Craig, F.E. Christensen, C.J. Hailey, m. more, The nuclear spectroscopic telescope array (nustar) high-energy x-ray mission, *Astrophys. J.* 770 (2013) 103.
- [19] M. Civitani, S. Basso, M. Ghigo, G. Pareschi, B. Salmaso, D. Spiga, G. Vecchi, R. Banham, E. Breuning, V. Burwitz, G. Hartner, B. Menz, Cold and Hot Slumped Glass Optics with interfacing ribs for high angular resolution x-ray telescopes, in: Space Telescopes and Instrumentation 2016: Ultraviolet to Gamma Ray, in: Proceedings of the SPIE, vol. 9905, 2016, p. 99056U, <http://dx.doi.org/10.1117/12.2232591>.
- [20] M. Tashiro, et al., Status of x-ray imaging and spectroscopy mission (XRISM), in: Space Telescopes and Instrumentation 2020: Ultraviolet to Gamma Ray, Vol. 11444, International Society for Optics and Photonics, 2020, p. 1144422, <http://dx.doi.org/10.1117/12.2565812>, URL <https://www.spiedigitallibrary.org/conference-proceedings-of-spie/11444/1144422>Status-of-x-ray-imaging-and-spectroscopy-mission-XRISM/10.1117/12.2565812.short>.
- [21] Y. Giomataris, P. Reboursard, J. Robert, G. Charpak, MICROMEGRAS: A high-granularity position-sensitive gaseous detector for high particle-flux environments, *Nucl. Instrum. Methods Phys. Res. A* 376 (1) (1996) 29–35, [http://dx.doi.org/10.1016/0168-9002\(96\)00175-1](http://dx.doi.org/10.1016/0168-9002(96)00175-1), URL <https://www.sciencedirect.com/science/article/pii/0168900296001751>.
- [22] S. Andriamonje, D. Attie, E. Berthoumieux, M. Calviani, P. Colas, T. Dafni, G. Fanourakis, E. Ferrer-Ribas, J. Galan, T. Geralis, A. Giganon, I. Giomataris, A. Gris, C.G. Sanchez, F. Gunsing, F.J. Igua, I. Irastorza, R.D. Oliveira, T. Papaevangelou, J. Ruz, I. Savvidis, A. Teixera, A. Tomás, Development and performance of microbulk micromegas detectors, *J. Instrum.* 5 (02) (2010) P02001, <http://dx.doi.org/10.1088/1748-0221/5/02/p02001>.
- [23] F. Aznar, J. Castel, F. Christensen, T. Dafni, T. Decker, E. Ferrer-Ribas, J. Garcia, I. Giomataris, J. Garza, C. Hailey, R. Hill, F. Igua, I. Irastorza, A. Jakobsen, G. Luzon, H. Mirallas, T. Papaevangelou, M. Pivovaroff, J. Ruz, T. Vafeiadis, J. Vogel, A micromegas-based low-background x-ray detector coupled to a slumped-glass telescope for axion research, *J. Cosmol. Astropart. Phys.* 2015 (12) (2015) 008, <http://dx.doi.org/10.1088/1475-7516/2015/12/008>.
- [24] C. Krieger, K. Desch, J. Kaminski, M. Lupberger, Operation of an InGrid based X-ray detector at the CAST experiment, *EPJ Web Conf.* 174 (2018) 02008, <http://dx.doi.org/10.1051/epjconf/201817402008>.
- [25] C. Ligtenberg, K. Heijhoff, Y. Bilevych, K. Desch, H. van der Graaf, F. Hartjes, J. Kaminski, P. Kluit, G. Raven, T. Schiffer, J. Timmermans, Performance of a GridPix detector based on the Timepix3 chip, *Nucl. Instrum. Methods Phys. Res. A* 908 (2018) 18–23, <http://dx.doi.org/10.1016/j.nima.2018.08.012>, URL <https://www.sciencedirect.com/science/article/pii/S0168900218309549>.
- [26] S. Mertens, A. Alborini, K. Altenmüller, T. Bode, L. Bombelli, T. Brunst, M. Carminati, D. Fink, C. Fiorini, T. Houdy, A. Huber, M. Korzeck, T. Lasserre, P. Lechner, M. Manotti, I. Peric, D.C. Radford, D. Siegmann, M. Slezák, K. Valerius, J. Wolf, S. Wüstling, A novel detector system for KATRIN to search for keV-scale sterile neutrinos, *J. Phys. G: Nucl. Part. Phys.* 46 (6) (2019) 065203, <http://dx.doi.org/10.1088/1361-6471/ab12fe>.
- [27] D. Unger, A. Abeln, C. Enss, A. Fleischmann, D. Hengstler, S. Kempf, L. Gastaldo, High-resolution for IAXO: MMC-based X-ray detectors, *J. Instrum.* 16 (06) (2021) P06006, <http://dx.doi.org/10.1088/1748-0221/16/06/p06006>.
- [28] S. Anvar, P. Baron, B. Blank, J. Chavas, E. Delagnes, F. Druillolle, P. Hellmuth, L. Nalpas, J. Pedroza, J. Pibernat, E. Pollacco, A. Rebii, N. Usher, AGET, the GET front-end ASIC, for the readout of the time projection chambers used in nuclear physic experiments, in: 2011 IEEE Nuclear Science Symposium Conference Record, 2011, pp. 745–749, <http://dx.doi.org/10.1109/NSSMIC.2011.6154095>.
- [29] K. Altenmüller, S. Cebrián, T. Dafni, D. Díez-Ibáñez, J. Galán, J. Galindo, J.A. García, I.G. Irastorza, G. Luzón, C. Margalejo, H. Mirallas, L. Obis, O. Pérez, K. Han, K. Ni, Y. Bedfer, B. Biasuzzi, E. Ferrer-Ribas, D. Neyret, T. Papaevangelou, C. Cogollos, E. Picatoste, REST-for-physics, a ROOT-based framework for event oriented data analysis and combined Monte Carlo response, *Comput. Phys. Comm.* 273 (2022) 108281, <http://dx.doi.org/10.1016/j.cpc.2021.108281>, URL <https://www.sciencedirect.com/science/article/pii/S0010465521003933>.